

## X-Ray Photoelectron Spectroscopy Study of $(\text{Ca}_{1-x}\text{La}_x)\text{MnO}_{2.97}$ ( $0.1 \leq x \leq 0.4$ )

H. TAGUCHI\*<sup>†</sup>

*Osaka Prefectural Industrial Research Institute, Nishi-Ku,  
Osaka 550, Japan*

AND M. SHIMADA

*Department of Applied Chemistry, Faculty of Engineering, Tohoku  
University, Sendai 980, Japan*

Received January 29, 1986; in revised form June 2, 1986

The X-ray photoelectron spectroscopy (XPS) of perovskite-type  $(\text{Ca}_{1-x}\text{La}_x)\text{MnO}_{2.97}$  ( $0.1 \leq x \leq 0.4$ ) was measured at room temperature. From the absolute values of the binding energy difference ( $\Delta\text{BE}$ ) of  $\text{Ca}2p\text{-O}1s$ ,  $\text{La}3d\text{-O}1s$ , and  $\text{Mn}2p\text{-O}1s$ , both the chemical bonding of Mn-O and Ca-O become more covalent, and that of La-O becomes more ionic with increasing  $x$ . The electron transfer of the Mn-O-Mn path is dominant, and the electrical properties are strongly influenced by the decrease of the electron transfer of the Mn-O-(Ca,La)-O-Mn path. © 1987 Academic Press, Inc.

### Introduction

$(\text{Ca}_{1-x}\text{La}_x)\text{MnO}_{2.97}$  ( $0 \leq x \leq 0.4$ ) has the perovskite-type structure and exhibits  $n$ -type semiconductor below room temperature (1). Below 125 K, the electrical resistivity follows the Mott's  $T^{-1/4}$  law indicating the possible occurrence of variable hopping of electrons due to Anderson localization (2, 3). Above ca. 400-450 K, a metal-insulator transition is encountered. From the results of DTA measurements, this transition occurs without the crystallographic change. On the other hand, the magnetic susceptibility has a deflection point at ca.

450-500 K. From the results of the electrical and magnetic measurements, the mechanism of the metal-insulator transition in these manganates is explained by the band model proposed by Goodenough (4).

Taguchi and Shimada measured the X-ray photoelectron spectroscopy (XPS) of perovskite-type  $\text{CaMnO}_{3-\delta}$  at room temperature (5). The binding energies of  $\text{Ca}2p_{1/2}$  and  $\text{Ca}2p_{3/2}$  slightly decrease with decreasing oxygen content. On the other hand, the binding energy of  $\text{O}1s_{1/2}$  increases with decreasing oxygen content. Since the spectrum of  $\text{Mn}2p_{3/2}$  is broad, the binding energy is independent of the oxygen content. From the results of the binding energy difference ( $\Delta\text{BE}$ ), the chemical bonding of Mn-O becomes more covalent, and that of Ca-O becomes more ionic with decreasing oxygen content. The electron transfer in the Mn-

\* To whom all correspondence should be addressed.

<sup>†</sup> Present address: Research Laboratory for Surface Science, Faculty of Science, Okayama University, Tsushima, Okayama 700, Japan.

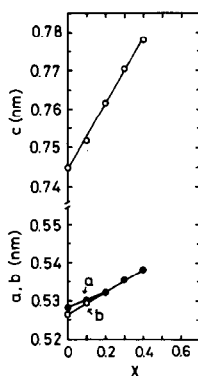


FIG. 1. Cell constants vs composition in the system  $(\text{Ca}_{1-x}\text{La}_x)\text{MnO}_{2.97}$ . (The cell constants of  $x = 0$  are given the values reported by Poppelmeier *et al.* (7))

O–Mn path can take place easily in the perovskite-type  $\text{CaMnO}_{3-\delta}$ .

In the present study, XPS of  $(\text{Ca}_{1-x}\text{La}_x)\text{MnO}_{2.97}$  ( $0.1 \leq x \leq 0.4$ ) is measured to examine the electron transfer from O1s to Ca2p, La3d and Mn2p. These results will provide information regarding the electrical properties of the perovskite-type manganates.

### Experimental

Samples were prepared using a standard ceramic technique. Powders of  $\text{CaCO}_3$ ,  $\text{La}_2\text{O}_3$ , and  $\text{MnCO}_3$  were weighed in the desired proportions and milled for a few hours with acetone. After the mixed powders were dried at  $100^\circ\text{C}$ , they were calcined in air at  $800^\circ\text{C}$ , then fired at  $1300^\circ\text{C}$  for 24 hr in a flow of pure oxygen gas. The oxygen-deficient materials obtained in this way were annealed at  $600\text{--}700^\circ\text{C}$  in air for 50 hr.

The phases of the samples were identified by X-ray powder diffraction with filtered  $\text{CuK}\alpha$  radiation. The cell constants of the samples were determined using Si as a standard material. The oxygen content in each sample was determined by the oxidation–reduction method (6). XPS measurements were carried out for Ca2p, La3d, Mn2p,

and O1s levels of the samples using  $\text{AlK}\alpha$  radiation ( $h\nu = 1486.6 \text{ eV}$ ) at room temperature. The energy calibration was made against the C1s peak from the usual contamination.

### Results and Discussion

X-ray powder diffraction patterns of all samples are completely indexed as the perovskite-type structure. The oxygen content of all samples annealed at  $600\text{--}700^\circ\text{C}$  in air is determined to be 2.97 ( $\delta = 0.03$ ) from the chemical analysis. The relation between the cell constants and the composition is shown in Fig. 1. In Fig. 1, the cell constants of  $x = 0$  are given the values of the single crystals reported by Poppelmeier *et al.* (7). The cell constants increase with increasing  $x$ , and the crystal structure changes from orthorhombic to tetragonal symmetry at  $x = 0.2$ . The tetragonal cell constants also increase with increasing  $x$  in the range  $0.2 \leq x \leq 0.4$ . Since the ionic radii of  $\text{Ca}^{2+}$  and  $\text{La}^{3+}$  ions are 0.132 and 0.135 nm, respectively (8), the monotonic increase in the cell constants is explained by the difference of the ionic radii between  $\text{Mn}^{3+}$  and  $\text{Mn}^{4+}$ .

The XPS of the Ca2p level of  $(\text{Ca}_{1-x}\text{La}_x)\text{MnO}_{2.97}$  is shown in Fig. 2. The binding energies of Ca2p<sub>1/2</sub> and Ca2p<sub>3/2</sub> slightly increase with increasing  $x$ . The satellite peaks on the high binding energy side of the Ca2p peaks are separated from the main peaks by ca. 1.2 eV, and this value is independent of the composition. In  $\text{CaMnO}_{3-\delta}$ , the energy difference between the Ca2p peak and the satellite peak increases from 1.2 to 2.0 eV with decreasing oxygen content (5). From these results, it is considered that the energy differences between the main peak and the satellite peak is strongly influenced by the oxygen content in the perovskite-type manganate.

Figure 3 shows the XPS of the La3d<sub>5/2</sub> level. The binding energy of La3d<sub>5/2</sub> slightly

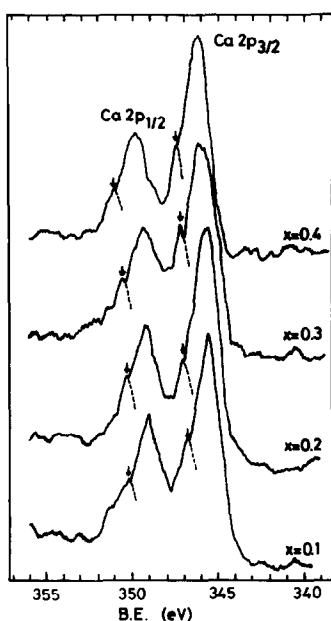


FIG. 2. XPS spectra of the  $\text{Ca}2p$  level in the system  $(\text{Ca}_{1-x}\text{La}_x)\text{MnO}_{2.97}$ .

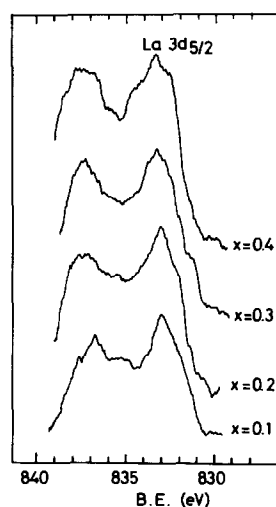


FIG. 3. XPS spectra of the  $\text{La}3d$  level in the system  $(\text{Ca}_{1-x}\text{La}_x)\text{MnO}_{2.97}$ .

increases with increasing  $x$ . The satellite peak on the high binding energy side of the  $\text{La}3d$  level is separated from the main peak by ca. 4 eV. Lam *et al.* reported the electronic structure of  $\text{LaBO}_3$  ( $B = \text{Ti}, \text{Cr}, \text{Mn}, \text{Fe},$  and  $\text{Co}$ ) using the XPS measurement (9). In the  $\text{La}3d$  spectra of  $\text{LaBO}_3$ , the satellite peaks are observed on the high binding energy side of the main peaks by ca. 4 eV. The satellite is interpreted in terms of the excitation of an electron from the anion valence band into the lanthanum  $f$  band. From these results, it is considered that the present satellite of the  $\text{La}3d$  peak in  $(\text{Ca}_{1-x}\text{La}_x)\text{MnO}_{2.97}$  is due to the excitation of the electron in analogy with  $\text{LaBO}_3$ .

Figure 4 shows the XPS of the  $\text{Mn}2p_{3/2}$  level. The  $\text{Mn}2p_{3/2}$  peak is broad and the binding energy is independent of the composition. The binding energy of  $\text{Mn}2p_{3/2}$  in  $\text{LaMn}^{3+}\text{O}_3$  and  $\text{Mn}^{4+}\text{O}_2$  is ca. 642.0 and 642.4 eV, respectively (9, 10). These values are also shown in Fig. 4. Kowalczyk *et al.*

reported that the  $\text{Mn}2p_{3/2}$  peak in  $\text{MnF}_2$  was broad and asymmetric toward the high binding energy site, and this asymmetry was discussed in terms of multiplet splitting

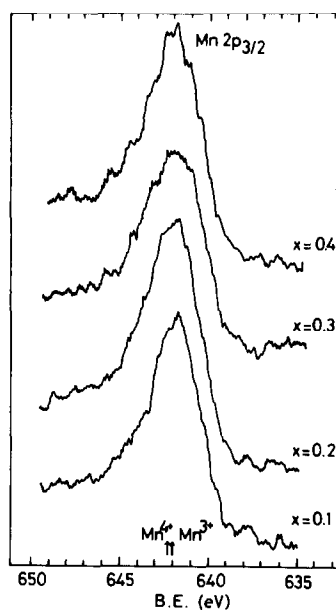


FIG. 4. XPS spectra of the  $\text{Mn}2p$  level in the system  $(\text{Ca}_{1-x}\text{La}_x)\text{MnO}_{2.97}$ .

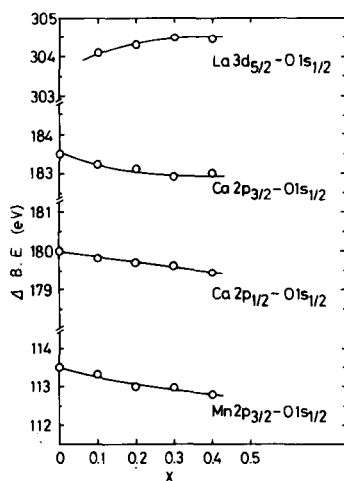


FIG. 5. Absolute values of the binding energy difference ( $\Delta BE$ ) of  $Ca2p-O1s$ ,  $La3d-O1s$ , and  $Mn2p-O1s$  in the system  $(Ca_{1-x}La_x)MnO_{2.97}$ .

(11). From these results, it is concluded that the present broad  $Mn2p_{3/2}$  peak in  $(Ca_{1-x}La_x)MnO_{2.97}$  is due to the mixed valency of both  $Mn^{3+}$  and  $Mn^{4+}$  ion and the multiplet structure in analogy with  $MnF_2$ .

The binding energy of  $O1s$  in  $(Ca_{1-x}La_x)MnO_{2.97}$  is ca. 529.1 eV, and this value slightly increases with increasing  $x$ . Figure 5 shows the absolute values of the binding energy difference ( $\Delta BE$ ) of  $Ca2p-O1s$ ,  $La3d-O1s$ , and  $Mn2p-O1s$ .  $\Delta BE$  of both  $Ca2p-O1s$  and  $Mn2p-O1s$  decreases with increasing  $x$ . On the other hand,  $\Delta BE$  of  $La3d-O1s$  increases with increasing  $x$ . Johnson reported that the binding energies of  $O1s_{1/2}$  in  $BeO$ ,  $MgO$ , and  $CaO$  were 532.1, 530.0 and 529.6 eV, respectively (12). The binding energy of  $O1s_{1/2}$  increases with increasing electronegativity of the alkaline earth metal ion. Carver *et al.* reported that the binding energies of  $Mn2p_{3/2}$  in  $MnO$ ,  $MnS$ ,  $MnF_2$ ,  $MnCl_2$ ,  $MnBr_2$ , and  $MnI_2$  were 641.7, 640.5, 642.8, 642.1, 642.2, and 642.1 eV, respectively (10). Since the electronegativity of the anion is as follows,  $O^{2-} > S^{2-}$ ,  $F^- > Cl^- > Br^- > I^-$ , it is

expected that the binding energy of  $Mn2p_{3/2}$  decreases with increasing covalency of the  $Mn-X$  ( $X = O, S, F, Cl, Br,$  and  $I$ ) bond. Citrin discussed the binding energy of  $Ru^{2+}$  and  $Ru^{3+}$  in  $[(NH_3)_5Ru(pyr)Ru(NH_3)_4]^{4+,5+,6+}$  salt from XPS measurements (13).  $Ru^{2+}$  and  $Ru^{3+}$   $3d$  electron binding energy in the  $[2+,3+]$  salt slightly converged with respect to those in the  $[2+,2+]$  and the  $[3+,3+]$  salts, and this convergence is understood in the results by the increase of the electron transfer between  $Ru^{2+}$  and  $Ru^{3+}$ . From these results, it is concluded that the chemical bonding of both  $Ca-O$  and  $Mn-O$  becomes more covalent with increasing  $x$ . On the other hand, the chemical bonding of  $La-O$  becomes more ionic with increasing  $x$ .

The electrical resistivity ( $\rho$ ) at room temperature and the activation energy ( $\Delta E$ ) of  $(Ca_{1-x}La_x)MnO_{2.97}$  are listed in Table I (1, 14). With increasing  $x$ , both  $\rho$  and  $\Delta E$  abruptly decrease and have minimum values at ca.  $x = 0.1$ , and then gradually increase. In the perovskite-type  $(Ca_{1-x}La_x)MnO_{2.97}$ , two paths of the electron transfer are considered. One is  $Mn-O-Mn$  and the other is  $Mn-O-(Ca,La)-O-Mn$ . Though the distance of  $Mn-O-Mn$  increases with increasing  $x$  as shown in Fig. 1, it is apparent from the results of XPS measurements that the chemical bonding of  $Mn-O$  becomes more covalent and the electron

TABLE I  
THE ELECTRICAL RESISTIVITY ( $\rho$ ) AT ROOM TEMPERATURE AND THE ACTIVATION ENERGY ( $\Delta E$ ) IN THE SYSTEM  $(Ca_{1-x}La_x)MnO_{2.97}$  (Refs. 1, 14)

$x$	$\log \rho_{\text{room temp.}} (\Omega \text{ cm})$	$\Delta E$ (eV)
0	2.98	ca. 3.0
0.05	-0.62	0.04
0.1	-0.94	0.05
0.2	-0.84	0.12
0.3	-0.76	0.18
0.4	-0.36	0.19

transfer of the Mn–O–Mn path is dominant. The chemical bonding of Ca–O becomes more covalent, but that of La–O becomes more ionic with increasing  $x$ . From these results, it is considered that the electron transfer in both Mn–O–Mn and Mn–O–(Ca,La)–O–Mn paths easily takes place in the range  $0 \leq x \leq 0.1$ . On the other hand, the electron transfer in the Mn–O–(Ca,La)–O–Mn path becomes difficult with increasing  $\text{La}^{3+}$  ion content. Consequently, both the electrical resistivity and the activation energy have minimum values at ca.  $x = 0.1$ .

It is concluded that the chemical bonding of both Mn–O and Ca–O becomes more covalent and that of La–O becomes more ionic with increasing  $x$  in the system  $(\text{Ca}_{1-x}\text{La}_x)\text{MnO}_{2.97}$ . The electron transfer of the Mn–O–Mn path is dominant and that of the Mn–O–(Ca,La)–O–Mn path decreases with increasing  $x$ . The electrical properties are strongly influenced by these two paths of electron transfer.

## References

1. H. TAGUCHI AND M. SHIMADA, *J. Solid State Chem.*, **63**, 290 (1986).
2. V. JOSHI, O. PARKASH, G. N. RAO, AND C. N. R. RAO, *J. Chem. Soc., Faraday Trans. II*, 75 (1979).
3. N. F. MOTT, *Adv. Phys.* **21**, 785 (1972).
4. J. B. GOODENOUGH, *J. Appl. Phys.* **37**, 1415 (1966).
5. H. TAGUCHI AND M. SHIMADA, *Phys. Status Solidi B* **131**, K59 (1985).
6. B. E. GUSHEE, L. KATZ, AND R. WARD, *J. Amer. Chem. Soc.* **79**, 5601 (1957).
7. K. R. POEPELMEIER, M. E. LEONOWICZ, J. C. SCANLON, J. M. LONGO, AND W. B. YELON, *J. Solid State Chem.* **45**, 71 (1982).
8. R. D. SHANNON AND C. T. PREWITT, *Acta Crystallogr. B* **25**, 925 (1969).
9. D. J. LAM, B. W. VEAL, AND D. E. ELLIS, *Phys. Rev. B* **22**, 5730 (1972).
10. J. C. CARVER, G. K. SCHERITZER, AND T. A. CARLSON, *J. Chem. Phys.* **57**, 973 (1972).
11. S. P. KOWALCZYK, L. LEY, F. R. MCFEELY, AND D. A. SHIRLEY, *Phys. Rev. B* **11**, 1721 (1975).
12. O. JOHNSON, *Chem. Scripta* **8**, 162 (1975).
13. P. H. CITRIN, *J. Amer. Chem. Soc.* **95**, 6472 (1973).
14. H. TAGUCHI, *Phys. Status Solidi A* **88**, K79 (1985).